Journal of Molecular Structure 990 (2011) 14–20

Contents lists available at ScienceDirect

Journal of Molecular Structure

journal homepage: www.elsevier.com/locate/molstruc

DFT, FT-Raman, FT-IR and FT-NMR studies of 4-phenylimidazole

M.T. Güllüoğlu [a], Y. Erdogdu [a,*], J. Karpagam [b], N. Sundaraganesan [b], Ş. Yurdakul [c]

[a] Department of Physics, Ahi Evran University, 40040 Kirsehir, Turkey
[b] Dept. of Physics (Engg.), FEAT, Annamalai University, A. Nagar 608 002, India
[c] Department of Physics, Gazi University, 06500 Ankara, Turkey

ARTICLE INFO

Article history:
Received 19 August 2010
Received in revised form 8 January 2011
Accepted 11 January 2011
Available online 22 January 2011

Keywords:
4-Phenylimidazole
FTIR
FT-Raman spectra
DFT
NBO
NMR

ABSTRACT

The experimental and theoretical vibrational spectra of 4-phenylimidazole (4-PI) were studied. The FT-IR, FT-Raman and FT-NMR spectra of 4-PI molecule was recorded in the powder form. The tautomeric, structural and spectroscopic analysis of the title molecule was made by using density functional harmonic calculations. For the title molecule, only one tautomeric form was found most stable structure by using B3LYP level with the 6-311G(d,p) and 6-311G++(d,p) as basis set. Selected experimental bands were assigned and characterized based on the scaled theoretical wave numbers by their total energy distribution (TED). Stability of the molecule arising from hyperconjugative interactions, charge delocalization has been analyzed using natural bond orbital (NBO) analysis. The results show that charge in electron density (ED) in the σ^* anti-bonding orbitals and E_2 energies confirms the occurrence of intermolecular charge transfer (ICT) within the molecule.

The isotropic chemical shifts computed by ^{1}H and ^{13}C NMR analysis also show good agreement with experimental observations. The theoretically predicted FTIR and FT-Raman spectra of the title molecule have been constructed.

1. Introduction

Imidazole is a heterocyclic compound of five-membered diunsaturated ring structure composed of three carbon atoms and two nitrogen atoms at nonadjacent positions. The simplest member of the imidazole family is imidazole itself, colorless to pale yellow crystalline solid with a weak amine like odor; soluble in water and alcohol, melts at 89 °C, boils at 256 °C. Imidazoles are poorly soluble in water generally, but are dissolved in organic solvents, such as chloroform, propylene, glycol, and polyethoxylated castor oil. Imidazole ring is found in histidine (an essential amino acid) and histamine, the decarboxylated compound from histamine. Some imidazole compounds inhibit the biosynthesis of ergo sterol, required in cell membrane in fungal. They have antibacterial, antifungal, antiprotozoal, and anthelmintic activity. Several distinct phenylimidazoles are therapeutically useful antifungal agents against either superficial or systemic infections. Thiabendazoles which have anthelmintic and antifungal properties are imidazole class compounds. Benzimidazole is a dicyclic compound having imidazole ring fused to benzene. Benzimidazole structure is a part of the nucleotide portion of vitamin B_{12} and the nucleus in some drugs such as proton pump inhibitors and anthelmintic agents. Imidazole has two nitrogen atoms. The one is slightly acidic, while the other is basic. Imidazole and its derivatives are widely used as intermediates in synthesis of organic target compounds including pharmaceuticals, agrochemicals, dyes, photographic chemicals, corrosion inhibitors, epoxy curing agents, adhesives and plastic modifiers [1,2].

In the present work, we report the results of theoretical and experimental (IR and Raman and NMR) spectra, conformational analysis and molecular orbital energies of 4-PI molecule along with NBO analysis. The spectroscopic properties of 4-PI have not yet been studied in detail to the best of our knowledge. Therefore, the present investigation was undertaken to study the vibrational spectra of 4-PI molecule completely and to identify the various normal modes with greater wavenumber accuracy. Density functional theory (DFT/B3LYP) calculations have been performed to support our wavenumber assignments. Furthermore, we interpreted the calculated spectra in terms of total energy distributions (TED's) and made the assignment of the experimental bands.

2. Experimental

The FT-IR spectrum of this molecule is recorded in the region 4000–400 cm^{-1} on IFS 66 V spectrophotometer using KBr pellet technique is shown in Fig. 1. The FT-Raman spectrum of 4-PI has been recorded using 1064 nm line of Nd:YAG laser as excitation wavelength in the region 50–3500 cm^{-1} on a Thermo Electron Corporation model Nexus 670 spectrophotometer equipped with

* Corresponding author. Tel.: +90 0 386 211 45 57; fax: +90 0386 211 45 00.
E-mail address: yusuferdogdu@gmail.com (Y. Erdogdu).

0022-2860/$ - see front matter © 2011 Elsevier B.V. All rights reserved.
doi:10.1016/j.molstruc.2011.01.001

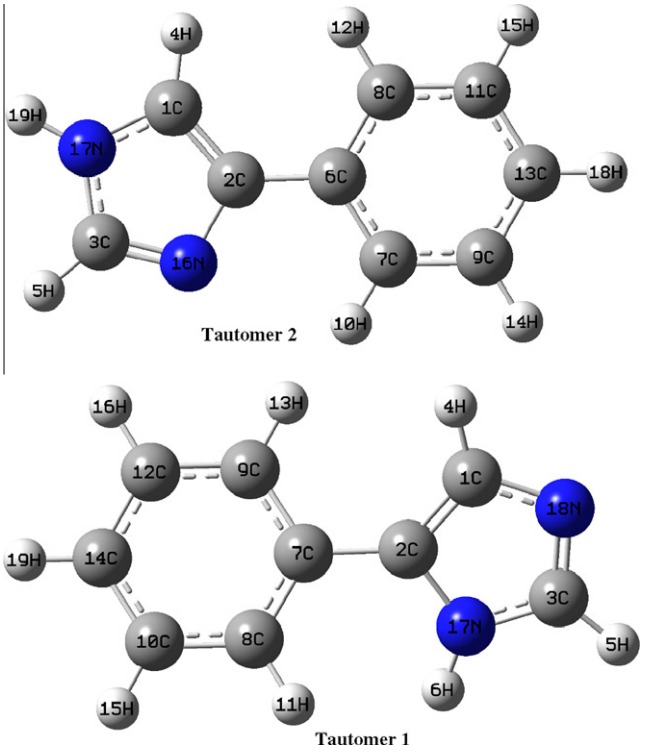

Fig. 1. Atom numbering scheme adopted in this study of 4-Phenylimidazole.

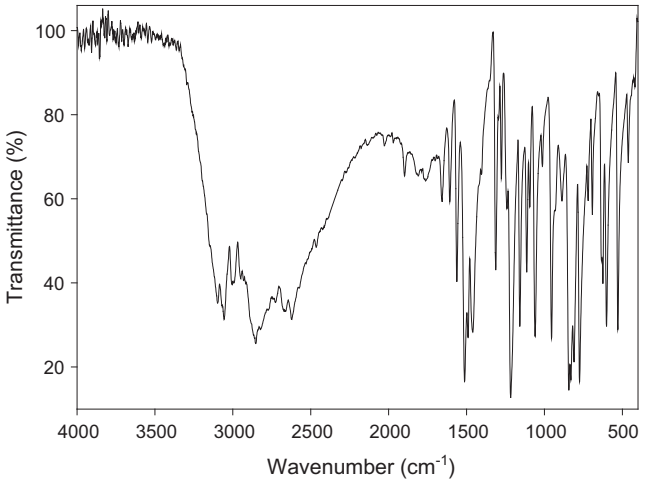

Fig. 2. FT-IR spectrum of 4-phenylimidazole.

FT-Raman module accessory are shown in Fig. 2. The ^{1}H and ^{13}C NMR spectra are taken in chloroform solutions and all signals are referenced to TMS on a BRUKER DPX-400 FT-NMR Spectrometer. All NMR spectra are measured at room temperature.

3. Computational details

Gaussian 03 quantum chemical software was used in all calculations [3]. The optimized structural parameters and vibrational wavenumbers for the 4-PI molecule were calculated by using B3LYP functional with 6-311G(d,p) and 6-311G++(d,p) as basis set. The vibrational modes were assigned on the basis of TED analysis using VEDA program [4]. The calculated vibrational wave numbers were scaled [5] with the scale factors in order to figure out how the calculated data were in agreement with those of the experimental ones.

Finally, the natural bonding orbitals (NBO) calculations [6] were performed using NBO 3.1 program as implemented in the Gaussian 03W package at the DFT/B3LYP level in order to understand various second order interactions between the filled orbitals of one subsystem and vacant orbitals of another subsystem, which is a measure of the intermolecular delocalization or hyper conjugation. NBO analysis provides the most accurate possible 'natural Lewis structure' picture of ø, because all orbital details are mathematically chosen to include the highest possible percentage of the electron density. It is shown that a useful aspect of the NBO method gives information about interactions in both filled and virtual orbital spaces that it could enhance the analysis of intra- and intermolecular interactions.

The second order Fock matrix was carried out to evaluate the donor–acceptor interactions in the NBO basis [7]. The interactions result in a loss of occupancy from the localized NBO of the idealized Lewis structure into an empty non-Lewis orbital. For each donor (i) and acceptor (j), the stabilization energy $E(2)$ associated with the delocalization $i \rightarrow j$ is estimated as

$$E_2 = \Delta E_{ij} = q_i \frac{F(i,j)^2}{\varepsilon_j - \varepsilon_i} \quad (1)$$

where q_i is the donor orbital occupancy, ε_i and ε_j are the diagonal elements and $F(i, j)$ is the off diagonal NBO Fock matrix element.

The ^{1}H and ^{13}C NMR chemical shifts calculations of the T2 tautomeric form of the 4-PI molecule were made by using B3LYP functional with 6-311G(d,p) and 6-311G++(d,p) basis set. The gauge including atomic orbital (GIAO) method is one of the most common approaches for calculating isotropic nuclear magnetic shielding tensors [8,9]. For the same basis set size GIAO method is often more accurate than those calculated with other approaches [10,11]. The NMR spectra calculations were performed by Gaussian 03 program package. The calculations reported were performed in chloroform solution using IEF-PCM model as well as gas phase in agreement with experimental chemical shifts obtained in chloroform solution.

3.1. Predictions of Raman Intensities

The Raman activities (S_i) calculated with Gaussian 03 program [3] converted to relative Raman intensities (I_i) using the following relationship derived from the intensity theory of Raman scattering [12,13].

$$I = \frac{f(v_o - v)^4 S_i}{v_i[1 - \exp(-hcv_i/kT)]} \quad (2)$$

where v_o is the exciting frequency in cm^{-1}, v_i the vibrational wavenumber of the ith normal mode, h, c and k are fundamental constants, and f is a suitably chosen common normalization factor for all peak intensities. For simulation, the calculated FT-Raman spectra were plotted using pure Lorentizian band shape with a bandwidth of full width and half maximum (FW–HM) of 10 cm^{-1}.

Gaussian 03 quantum chemical software was used in all calculations [22]. The optimized structural parameters and vibrational wavenumbers for all molecules were calculated by using B3LYP functional with 6-311G(d,p) and 6-311G++(d,p) basis set. The vibrational modes were assigned on the basis of potential energy distributions (PED) analysis using VEDA 4 program [23] and its visualization interface. Normal coordinate analysis of the title molecules has been carried out to obtain a more complete description of the molecular motions involved in the fundamentals. The calculated harmonic vibrational wavenumbers were scaled down uniformly by a factor of 0.9613 (B3LYP/6-311G(d,p)) and 0.967 (for

wave numbers under 1800 cm^{-1}) and 0.955 (for those over 1800 cm^{-1}) for B3LYP/6-311++G(d,p) level of theory, which accounts for systematic errors caused by basis set incompleteness, neglect of electron correlation and vibrational anharmonicity [23].

4. Results and discussion

4.1. Molecular structure

The optimized tautomeric forms of 4-PI is shown Fig. 3. Many attempts to investigate the tautomeric equilibrium structure of this molecule have been made using different calculation methods. It is determined that T2 is more stable than T1 by 3 kJ mol^{-1} for AM1 and PM3 calculations by Ögretir and Yarligan [15]. Maye and Venanzi have calculated rotational barrier and energies of both T2 and T1 tautomeric forms of 4-PI [16]. They reported that the difference in energy is 7.5 kJ mol^{-1} by T2 compared with T1. In the present work, we determined that the energy of tautomers of 4-PI are −457.389989677 (T1) and −457.391997655 (T2) by B3LYP/6-311G(d,p) level of theory. Theoretically we find that T2 is more stable than T1 by 5.27 kJ mol^{-1} by B3LYP/6-311G(d,p) level of theory.

The optimized bond lengths and bond angles of the T2 tautomeric form of the 4-PI molecule at B3LYP/6-311G(d,p) level is collected in Table S1. These optimized geometric parameters of 4-PI are compared with those of X-ray data [14]. The order of the optimized bond lengths of six C–C bonds of the benzene ring are in ascending order as C_7–C_9, C_8–C_{11}, C_9–C_{13}, C_{11}–C_{13}, C_6–C_7 and C_6–C_8. The C_6–C_7 and C_6–C_8 bond lengths for 4-PI exactly at the substitution approximately equal as well as slightly longer than other C–C bond lengths. The bond angle C_7–C_6–C_8 exactly at the substitution is 118° which is slightly lower than hexagonal structure. The optimized N–H bond length for benzimidazole is 1.008 Å by B3LYP method. Our predicted N–H bond length for 4-phenyl imidazole is 1.007 Å which. The interaction of the imidazole ring on the benzene ring is of great importance in determining its structure and vibrational properties. The imidazole ring moiety is essentially out-of-plane with benzene ring as evident from torsional angles [C_1–C_2–C_6–C_7 = −151° and C_1–C_2–C_6–C_8 = 28°].

The aim of the conformational analysis of the 4-PI molecule is to provide a model for the molecular structure. The T2 and T1 tautomeric forms of 4-PI molecule were calculated, the energy barrier of rotation around the bond C_6–C_2 by B3LYP/6-311G(d,p) level of theory. The dihedral angle N_{16}–C_2–C_6–C_7 (around C_6–C_2 bond) was varied form 0° to 180° by steps of 10°. Then, the optimized molecular structure and vibrational normal modes were calculated for ground state in the B3LYP with 6-311G(d,p) basis sets.

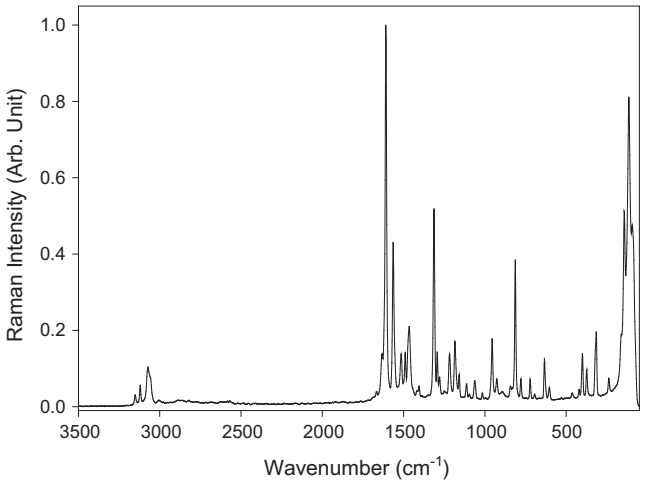

Fig. 3. FT-Raman spectrum of 4-phenylimidazole.

The variation of rotational barriers with the dihedral angles were shown in Fig. S1. The molecular geometry was defined through two effects acting oppositely: a repulsion of the hydrogen atoms in *ortho* positions on the ring, which would lead to a staggered conformation of the molecule, and a conjugation effect, which tends to bring phenyl ring in the imidazole plane. The equilibrium geometry of the molecule results from a balance between these two effects.

The variation of rotational barriers showed a double-well potential when the dihedral angle varies form 0° to 180°. The two minima occurring at variation of the torsional angles were identical. For this reason, it was satisfactory to optimize only one of the two equivalent minima. These minimums was determined α and $180 - \alpha$ firstly and second equivalent minima, respectively. Where α was designated N_{16}–C_2–C_6–C_7 dihedral angles.

It was reported that T2 tautomeric form was planar (N_{16}–C_2–C_6–C_7 dihedral angle for 0°) and T1 tautomeric form was twisted (N_{16}–C_2–C_6–C_7 dihedral angle for 35.3°) by Maye and Venanzi [16]. The T2 tautomeric form predicted a near planar equilibrium structure and the dihedral angle between phenyl and imidazole ring is 9° for HF/6-31G(d) level of theory [17]. Thus, we predicted at 26.45° T1 tautomeric form (N_{16}–C_2–C_6–C_7 dihedral angle) and 0° T2 tautomeric form (N_{16}–C_2–C_6–C_7 dihedral angle) by B3LYP/6-311G(d,p) level of theory.

4.2. Vibrational analysis

The 4-PI molecule consists of 19 atoms, which has 51 normal modes. The 51 normal modes of 4-PI have been assigned according to the detailed motion of the individual atoms. This molecule belongs to C_1 symmetry group. To the best of our knowledge, there is no detailed quantum chemical study for the molecular structure and vibrational spectra of 4-PI. Scale factors are used to fit the calculated wavenumbers with those of the observed ones. The experimental FT-IR and FT-Raman wavenumbers are tabulated in Table 1 together with the calculated wavenumbers. As seen in tables IR absorption intensities of 4-PI are in consistency with the PED results.

4.2.1. C–H vibrations

The assignments of carbon–hydrogen stretching modes are straight forward on the basis of the scaled ab initio predicted frequencies as well known "group frequencies". The aromatic structure shows the presence of the C–H stretching vibrations in the region 3100–3000 cm^{-1} which is the characteristic region for the ready identification of the C–H stretching vibrations [18]. In this region, the bands are not affected appreciably by the nature of the substituents. The 4-PI has five C–H moieties correspond to aromatic ring stretching and two C–H moieties to the imidazole ring as shown in Fig. 3. The expected five C–H stretching of the benzene ring corresponds to (mode nos. 48–44) stretching modes of C_7–H, C_8–H, C_9–H, C_{11}–H and C_{13}–H units. The vibrational mode nos. 48–44 are assigned to C–H stretching mode of aromatic ring computed by B3LYP/6-311G(d,p) method at 3052–3097 cm^{-1} show good agreement with recorded FT-IR and FT-Raman data at 3052, 2992 cm^{-1} and 3061 and 2922 cm^{-1} respectively. They are pure modes since their TED contribution is almost gives rise to ∼98%. Pyridine and its derivatives show the presence of C–H stretching vibrations in the region 3120–3010 cm^{-1} which is the characteristic region for the ready identification of C–H stretching vibrations [19,20]. For benzimidazole ring the C–H stretching mode is observed at 3111 cm^{-1} by Castillo et al. [21]. Our theoretically computed wavenumbers for the imidazole ring falls within the range of 3134–3163 cm^{-1} corresponding to the stretching modes of C_1–

Table 1
Vibrational frequencies of 4-PI for B3LYP methods with 6-311G(d.p) and 6-311++G(d.p).

Mode nos	Tautomer 1				Tautomer 2				Exp. IR	Exp. RA	TED[e]%
	6-311G(d,p)	6-311++G(d,p)			6-311G(d,p)	6-311++G(d,p)					
	Freq[a]	Freq[b]	I_{IR}[c]	I_{Raman}[d]	Freq[a]	Freq[b]	I_{IR}[c]	I_{Raman}[d]			
1	53	50	5.34	4.16	31	24	4.46	0.02		62	Γ_{CCCN}(95) P-IMI
2	102	101	0.55	0.39	109	108	5.84	0.23			Γ_{CCCC}(55) + γ_{CNCC}(35) P-IMI
3	134	135	2.59	0.34	156	156	5.22	0.02		143	δ_{CCC}(76) + γ_{CNCC}(12) P-IMI
4	279	277	1.45	0.42	278	274	4.18	0.57		307	Γ_{CCCC}(29) P + Γ_{CCCC}(15) + γ_{CNCC}(22) P-IMI
5	335	335	0.13	31.5	341	341	0.22	40.5		346	ν_{CC}(34) P-IMI + δ_{CCN}(13) IMI + δ_{CCC}(21) P
6	400	398	0.04	3.54	398	396	0.01	0.02		404	Γ_{HCCC}(23) + Γ_{CCCC}(66) P
7	410	409	3.26	8.06	433	432	3.70	13.7	433	431	δ_{CCC}(58) P-IMI
8	497	492	12.4	4.47	493	482	100	2.01			Γ_{HNCN}(13) IMI + Γ_{CCCC}(32) P
9	523	515	100	4.04	507	496	7.87	3.38	521	521	Γ_{HNCN}(71) IMI
10	613	612	0.52	9.97	614	613	0.00	14.7	598	618	δ_{CCC}(78) P
11	652	646	5.42	5.22	631	623	2.97	0.52	632	631	Γ_{HNCN}(13)+Γ_{HCNC}(11) + Γ_{CCNC}(14) + Γ_{NCNC}(53) IMI
12	659	653	3.99	1.82	674	673	9.92	9.68			Γ_{HCNC}(14)+Γ_{CCNC}(50)+Γ_{NCNC}(13) + γ_{CNCC}(10) IMI
13	673	672	7.14	6.61	677	674	9.57	0.36			ν_{CC}(11) P-IMI + δ_{CCN}(11) P + δ_{CCC}(52) IMI
14	687	683	43.9	0.22	687	684	20.0	0.01	699	681	Γ_{HCCC}(40) + Γ_{CCCC}(57) P
15	751	748	54.2	4.32	719	719	67.0	1.22	760	760	Γ_{HCCC}(40) + Γ_{CCCC}(41) P
16	786	780	33.9	2.38	771	769	23.7	3.05	787	787	Γ_{HCNC}(82) + Γ_{NCNC}(16) IMI
17	822	819	3.23	6.39	799	790	21.7	3.39	842	849	Γ_{HCCC}(76) P
18	828	824	12.2	1.84	825	823	0.00	0.09			Γ_{HCNC}(72) IMI
19	893	890	3.66	0.17	900	899	3.47	0.05	895	895	Γ_{HCCC}(83) + Γ_{CCCC}(10) P
20	899	897	12.7	5.47	911	910	12.8	21.2	919		δ_{CNC}(66) IMI
21	945	945	8.13	26.6	921	920	3.15	4.53			Γ_{HCCC}(72) P
22	947	947	3.58	3.75	946	949	0.16	0.05	958	957	δ_{NCN}(35) IMI
23	969	965	0.14	0.27	973	969	0.34	0.35			Γ_{HCCC}(72) + Γ_{CCCC}(16) P
24	981	980	0.21	52.3	983	982	0.72	66.2	986		ν_{CC}(11) + δ_{CCC}(65) P
25	1014	1013	1.26	6.72	1013	1012	6.25	10.8	1009	1000	ν_{CC}(43) P
26	1045	1044	28.0	0.88	1043	1041	15.5	2.15	1024	1046	δ_{NCN}(20) + δ_{HNC}(14) + δ_{HCN}(13) IMI
27	1067	1067	6.12	0.47	1062	1061	5.71	0.92	1062		ν_{CC}(33) + δ_{HCC}(29) P
28	1083	1082	30.6	0.24	1081	1078	44.0	6.41			ν_{NC}(45) + δ_{HNC}(24) + δ_{HCN}(14) IMI
29	1118	1117	33.9	20.6	1094	1092	8.23	11.1	1109	1113	ν_{NC}(56) + δ_{HCN}(15) IMI
30	1144	1144	0.30	3.86	1142	1142	0.19	4.80	1157	1154	δ_{HCC}(76) P
31	1167	1167	1.37	9.29	1163	1163	0.41	8.35	1183	1181	δ_{HCC}(76) P
32	1214	1214	2.26	7.08	1195	1194	4.00	4.12	1226	1225	ν_{CC}(11) + δ_{HCN}(51) IMI
33	1264	1263	7.77	9.33	1257	1255	9.03	18.6	1261	1258	ν_{NC}(28) + δ_{HCN}(16) IMI
34	1271	1271	0.37	6.32	1288	1287	6.56	19.2	1284	1281	ν_{CC}(26) P + δ_{HCN}(14) IMI
35	1309	1309	0.73	1.36	1309	1307	0.63	29.0	1309	1310	ν_{CC}(22) + δ_{HCC}(55) P
36	1333	1332	10.1	47.4	1317	1317	1.29	1.78	1335	1333	ν_{NC}(22) + δ_{CCN}(19) IMI
37	1377	1375	19.6	24.2	1406	1400	18.0	57.3			ν_{CC}(13) + ν_{NC}(21) + δ_{HNC}(34) IMI
38	1419	1418	3.98	47.8	1430	1428	9.71	0.25	1395		ν_{NC}(28) + δ_{HCN}(11) IMI + δ_{HCC}(23)
39	1446	1444	23.5	30.6	1464	1460	6.85	8.09	1422	1441	ν_{CC}(11) + δ_{HCN}(13) + δ_{HCC}(14) IMI
40	1475	1473	30.3	4.38	1486	1483	39.3	5.59	1465	1466	δ_{HCC}(55) P
41	1548	1546	5.80	39.4	1533	1530	0.45	79.1	1558	1555	ν_{CC}(24) P + ν_{CC}(13) P-IMI
42	1566	1564	5.04	11.2	1569	1566	0.97	5.78	1579	1580	ν_{CC}(43) IM
43	1594	1590	34.4	100	1595	1592	19.2	100	1606	1607	ν_{CC}(28) IMI
44	3053	3016	10.0	0.63	3052	3016	4.45	0.86	2992	2992	ν_{CH}(91) P
45	3062	3024	0.03	1.93	3060	3023	3.33	3.37	3052	3061	ν_{CH}(78) P
46	3071	3033	16.8	2.17	3069	3032	31.2	1.73			ν_{CH}(98) P
47	3080	3042	23.9	0.81	3081	3043	21.2	6.90			ν_{CH}(90) P
48	3088	3049	11.9	6.83	3097	3058	3.38	3.09			ν_{CH}(98) P
49	3131	3095	4.73	1.17	3134	3097	2.52	3.62			ν_{CH}(100) IMI
50	3135	3099	2.44	2.83	3163	3125	0.75	1.77			ν_{CH}(99) IMI
51	3532	3488	53.4	0.83	3533	3489	88.6	3.65	3119	3119	ν_{NH}(100) IMI

[a] Scaling factor: 0.961 for B3LYP/6-311G(d,p).
[b] Obtained from the wave numbers calculated at B3LYP/6-311++G(d,p) using scaling factors 0.967 (for wave numbers under 1800 cm^{-1}) and 0.955 (for those over 1800 cm^{-1}).
[c] Relative absorption intensities normalized with highest peak absorption equal to 100.
[d] Relative Raman intensities calculated by Eqn (2) and normalized to 100.
[e] Total energy distribution calculated B3LYP 6-311G(d,p) level, TED less than 10% are not shown.

H and C_3–H moieties. All the aromatic C–H stretching bands are found to be weak and this is due to decrease of dipole moment caused by reduction of the negative charge on the carbon atom. This reduction occurs because of the electron withdrawal on the carbon atom by substituent due to the decrease of inductive effect, which in turn by the increase in chain length of the substituent [22].

The C–H in-plane bending vibrations appear in the range 1300–1000 cm^{-1} and out-of-plane bending vibrations occur in the range 1000–750 cm^{-1} for substituted benzenes [23]. In our title molecule weak to medium bands observed in FT-IR as well as in FT-Raman spectrum at 1309, 1183, 1157, 1062 cm^{-1} and 1310, 1181, 1154 cm^{-1} are assigned to C–H in-plane bending vibrations for aromatic ring show good agreement with computed wavenumbers at 1309, 1163, 1142 and 1062 cm^{-1}(mode nos. 35, 31, 30 and 27) by B3LYP/6-311G(d,p) method. The C–H in-plane bending vibrations correspond to the imidazole ring also falls within the range 1000–1400 cm^{-1} [21]. In our molecule the frequencies computed by B3LYP/6-311G(d,p) method at 1257 and 1195 cm^{-1} (mode nos. 33 and 32) are assigned to C–H in-plane bending vibration

of imidazole ring which mixes with the C–C, C–N stretching vibrations. For both rings, the C–H in-plane bending vibrations are not a pure more as it is evident from the Table 1. The medium band observed in FT-IR spectrum at 895 cm^{-1} and their counter part of FT-Raman also show the same magnitude but weak in intensity are assigned to C–H out-of-plane bending vibrations for the phenyl ring. The computed TED corresponds to this vibrations are almost contributing to 83%. The theoretically computed wavenumbers for these vibrations falls within in the range of 822–799 cm^{-1} (mode nos. 18–16).

4.2.2. N–H vibrations

The heteroaromatic molecule containing an N–H group and, its stretching absorption occur in the region 3500–3220 cm^{-1}. The position of absorption in this region depends upon the degree of hydrogen bonding, and hence upon the physical state of the sample or the polarity of the solvent [24]. Primary amines examined in dilute solution display two weak absorption bands, one near 3500 cm^{-1} and the other near 3400 cm^{-1}. These bands represent, respectively the asymmetric and symmetric N–H stretching modes [25]. The N–H stretching band of benzimidazole and 2-methylbenzimidazole were observed in the region 3460–3450 cm^{-1} [21]. In the present work, the theoretical calculation indicate the scaled frequency value at 3533 cm^{-1} (mode no. 51) is assigned to N–H stretching vibrations. The TED corresponds to this vibration is a pure mode with contribution of 100%, but the recorded spectra fails to shows such kind of band in the above said region, but it is observed at 3119 cm^{-1} in both spectra as a medium band is assigned to N–H stretching vibrations. The lower in frequencies in solid phase may be attributed due to presence of intermolecular hydrogen bonding, this results also well in agreement with our previous work of 3,5-dimethylpyrazole [26]. The presence of N–H out-of-plane bending vibration in free benzimidazole was observed at 433 cm^{-1} and 421 cm^{-1} for 2-methylbenzimidazole [21], the strong band observed in FT-IR spectrum at 521 cm^{-1} is assigned to N–H out-of-plane bending vibration show good agreement with computed wavenumber at 507 cm^{-1} (mode no. 9), the TED corresponding to this vibration is a pure mode of contributing to 71%. The N–H in-plane bending vibration computed by B3LYP/6-311G(d,p) method show good agreement with recorded spectral data.

4.2.3. Phenyl ring vibrations

The ring carbon–carbon stretching vibration occurs in the region 1625–1430 cm^{-1}. In general, the bands are of variable intensity are observed at 1625–1590, 1590–1575, 1540–1470, 1430–1465 and 1380–1280 cm^{-1} from the frequency ranges given by Varsanyi [19] for the five bands in the region. In the present study, the frequencies observed in the FT-IR spectrum at 1558, 1422, 1309, 1284, 1226 cm^{-1} are assigned to C–C stretching vibrations. The same vibrations appear in the FT-Raman spectrum at 1555, 1441, 1310, 1281, 1225 cm^{-1}. The computed wavenumber for C–C stretching vibrations are found with in the range 1533, 1464, 1309, 1288, 1195 cm^{-1} (mode nos. 41, 39, 35, 34, 32) by B3LYP/6-311G(d,p) method. The TED corresponding to these vibrations is a mixed mode of contributing less than 50%.

In the benzene, fundamental (992 cm^{-1}) and (1010 cm^{-1}) represent the ring breathing and carbon trigonal bending modes respectively. Under the C_s point group symmetry both the vibrations are very close, there is an appreciable interaction between these vibrations and consequently their energies will be modified. The ring breathing mode of 4-PI are assigned at 1009 cm^{-1} in FT-IR and, 1000 cm^{-1} as a very strong band in FT-Raman. The medium strong band at 986 cm^{-1} in FT-IR spectrum as trigonal bending mode. The theoretically computed values at 1013 and 983 cm^{-1} by B3LYP/6-311G(d,p) method exactly coincide with experimental observations. The in-plane deformation vibrations are at higher frequencies than out-of-plane vibrations. Shimanouchi et al. [27] gave the frequency data for these vibrations for different benzene derivatives as a result of normal coordinate analysis. For aromatic ring, some bands are observed below 700 cm^{-1}, these bands are quite sensitive to change in the nature and position of the substituents [28–31]. Although other bands depend mainly on the substitution and the number of substituent rather than on their chemical nature or mass, so that these latter vibrations, together with the out-of-plane vibrations of the ring hydrogen atoms are extremely useful in determining the positions of substituents. Two bands usually observed are those due to the in-plane and out-of-plane vibration and is generally weak for mono and para substituted benzenes. They are often masked by other strong absorptions which may occur due to the substituent group [32]. Considering the above factors, in our present study strong band observed in FT-IR spectrum at 598 cm^{-1} and 433 cm^{-1} as a weak band and 631, 404, 346 cm^{-1} as a weak to medium bands in FT-Raman spectrum are assigned to C–C–C in-plane and out-of-plane bending vibrations respectively. The computed wavenumber for the above said vibrations are also show consistent agreement with experimental observations.

4.2.4. Imidazole ring vibrations

The identifications of C═N, C—N vibrations is a difficult task, since the mixing of several bands are possible in the region. Silverstein et al. [32] assigned C═N stretching absorption in the region 1382–1266 cm^{-1} for aromatic amines. In benzamide the band observed at 1368 cm^{-1} is assigned to C═N stretching [33]. In benzotriazole, the C–N stretching band is found to be present at 1382 and 1307 cm^{-1}. In the present work, the FT-IR band observed at 1395 cm^{-1} have been assigned to C–N stretching vibrations of 4-PI. The predicted value of C–N stretching vibrations are at 1430, 1406 cm^{-1} (mode nos. 38–37). In addition to these the C–N–C, N–C–N, C–C–N bending vibrations (i.e. in-plane and out-of-plane) have been assigned by TED shows good agreement with recorded spectral data.

5. NBO analysis

Natural bond orbital analysis provides an efficient method for studying intra- and intermolecular bonding and interaction among bonds, and also provides a convenient basis for investigating charge transfer or conjugative interaction in molecular systems. Some electron donor orbital, acceptor orbital and the interacting stabilization energy resulted from the second-order micro-disturbance theory are reported [34–35]. The larger the $E(2)$ value, the more intensive is the interaction between electron donors and electron acceptors, i.e. the more donating tendency from electron donors to electron acceptors and the greater the extent of conjugation of the whole system. Delocalization of electron density between occupied Lewis-type (bond or lone pair) NBO orbitals and formally unoccupied (antibond or Rydgberg) non-Lewis NBO orbitals correspond to a stabilizing donor–acceptor interaction. NBO analysis has been performed on the molecule at the B3LYP/6-311G(d,p) level in order to elucidate the intramolecular, rehybridization and delocalization of electron density within the molecule. The intramolecular interaction are formed by the orbital overlap between bonding (C–C) and (C–C) antibond orbital which results intramolecular charge transfer (ICT) causing stabilization of the system. These interactions are observed as increase in electron density (ED) in C–C anti-bonding orbital that weakens the respective bonds. The electron density of six conjugated single bond of aromatic ring (~1.6e) clearly demonstrates strong delocalization. The strong intramolecular hyper conjugative interaction of the σ

electron of (C_1–C_2) distribute to $\sigma^*(C_1–H_4)$, $C_1–N_{18}$, $H_6–N_{17}$ and $C_7–C_8$ of the ring 2 to ring 1 leading to stabilization of ~4 kJ/mol are shown in Table S2. On the other hand, side the π (C_1–C_2) in the ring 2 further conjugate to the anti-bonding orbital of $\pi^*C_3–N_8$ and $\pi^*C_7–C_8$ which leads to strong delocalization of 16.05, 12.32 kJ/mol.

The π electron delocalization is maximum around $C_1–C_2$, $C_3–N_{18}$, $C_7–C_8$, $C_9–C_{12}$, $C_{10}–C_{14}$ of the ring 1 and 2 wich revealed by the ED at the five conjugated π (~1.7e) distributed to π^* bonding of $C_3–N_8$, $C_7–C_8$, $C_1–C_2$, $C_9–C_{12}$, $C_{10}–C_{14}$ which leads to stabilization of ~20 kJ mol^{-1}. These intramolecular charge transfer ($\sigma \rightarrow \sigma^*$, $\pi \rightarrow \pi^*$) can induce large nonlinearity of the molecule. The most important interaction energy in this molecule, is electron donating from N_{17} LP (1) to the anti-bonding ($C_1–C_2$) and $C_3–N_{18}$ resulting stabilization of 32.12 and 45.49 kJ mol^{-1}, respectively. As for the N_{18} LP(1) concerned the results indicate the less stabilization energy of 0.93 and 7.94 kJ mol^{-1} to the $C_1–C_2$ and $C_3–N_{17}$.

6. NMR spectra

The isotropic chemical shifts are frequently used as an aid in identification of reactive ionic species. It is recognized that accurate predictions of molecular geometries are essential for reliable calculations of magnetic properties. The NMR spectra calculations were performed for chloroform ($CDCl_3$) and in dimethylsulfoxide (DMSO) solvent. It is necessary to consider the solvent effects because the spectral data available are obtained in different solutions. The isotropic shielding values were used to calculate the isotropic chemical shifts δ with respect to tetramethylsilane (TMS) ($\delta^X_{iso} = \sigma^{TMS}_{iso} - \sigma^X_{iso}$). The values of σ^{TMS}_{iso} are 182.46 and 31.88 ppm for C and H NMR spectra, respectively.

The NMR spectra of imidazole and its derivative have been reported by several authors [36–39]. The NMR spectra of 4-phenylimidazole was determined in the DMSO-d_6 solution by Koskinen [38]. Koskinen reported list of chemical shifts without assignments. Claramunt et al. [14] reported the ^{1}H, ^{13}C and ^{15}N NMR spectra of 4-PI with different solutions. We experimentally reported ^{13}C and ^{1}H NMR spectra of 4-PI with chloroform solution. The range of the ^{13}C NMR chemical shifts for a typical organic molecule usually is >100 ppm [40–42] and the accuracy ensures reliable interpretation of spectroscopic parameters. In the present paper, the ^{13}C NMR chemical shifts for the title molecule are >100 ppm, as they would be expected. The computed chemical shifts as well as experimental NMR values are shown in Table 2.

The ^{13}C NMR chemical shift of C_2 observed larger than other carbons of imidazole group whereas C_1 chemical shift is lower than all other observed. This C_2 chemical shift is determined at 145.1 ppm (B3LYP/6-311G(d,p) level of theory), 135.6 ppm (experimental) and 138.7 ppm [14]. The C_1 chemical shift experimentally determined at 114.1 ppm in $CDCl_3$ solution. This shift observed at 115.2 ppm in $CDCl_3$ solution [14]. The computed C_1 chemical shift is found at 115.0 ppm. The C_1 chemical shift show consistent agreement with experimental data. They reported that C_3 chemical shift is greater than those of C_6 in some solution and imidazole derivatives, while different solution and imidazole derivatives C_6 chemical shift is greater than those of C_3 [14]. It was determined that the C_3 and C_6 chemical shifts of 4-PI molecule observed at 135.5 ppm and 133.0 ppm in $CDCl_3$ solution by Claramunt e al. [14], respectively. 1-methyl-4-phenylimidazole molecule observed at 137.9 ppm (for C_3 carbon) and 133.6 ppm (for C_6 carbon) in CDCl3 solution [37]. The C_3 chemical shift observed at 137.9 ppm (for 1-methyl-4-phenylimidazole), 138.1 ppm (for 1-methyl-5-phenylimidazole) and C_6 chemical shift observed at 134.3 ppm (for 1-methyl-4-phenylimidazole), 130.3 ppm (for 1-methyl-5-phenylimidazole) in $CDCl_3$ solution [40]. We calculated at 137.8 ppm (for C_3 carbon) and 139.3 ppm (for C_6 carbon) in $CDCl_3$ solution by B3LYP/6-311G(d,p) level of theory. The C_3 and C_6 chemical shifts of 4-PI molecule are experimentally observed at 129.0 ppm and 130.8 ppm in $CDCl_3$, respectively.

In the present work, we experimentally determined that the differences between C_6 and *meta* and *ortho* carbons of phenyl group are at 3.9 ppm and 9.5 ppm. These differences predicted at 7.2 ppm and 12.2 ppm for B3LYP/6-311G(d,p) level of theory. These differences were determined at 4.3 ppm and 8.1 ppm in $CDCl_3$ solution by Claramunt et al.

The protons of imidazole group were observed at 7.70 ppm, 7.59 ppm in the DMSO solution and 7.70 ppm, 7.35 ppm in the $CDCl_3$ solution [14]. We determined theoretically at 7.64 ppm, 7.60 ppm for B3LYP/6-311G(d,p) level of theory and experimentally at 7.74 ppm, 7.72 ppm in $CDCl_3$ solution. Calculated ^{1}H NMR peaks are agreement with those of both experimental and literature data.

Table 2
Theoretical and experimental ^{1}H and ^{13}C spectra of the all tautomers of 4-PI molecule (with respect to TMS, all values in ppm).

	B3LYP (theoretical)							Experimental	
	Tautomer 1			Tautomer 2		Average 6-311G(d,p)[a]	Average 6-311++G(d,p)[b]	New exp.	Exp. [14]
	6-311G(d,p)	6-311++G(d,p)		6-311G(d,p)	6-311++G(d,p)				
C_3	138.49	141.02	C_2	144.45	146.71	141.47	143.86	135.6	138.7
C_2	137.04	139.26	C_6	139.33	140.59	138.18	139.92	130.8	133.0
C_7	135.28	136.09	C_3	137.58	139.03	136.43	137.56	129.0	135.5
C_{10}	133.33	134.20	C_9	132.58	133.40	132.95	133.8	126.9	128.7
C_{12}	133.19	133.99	C_{11}	132.47	133.28	132.83	133.63	126.9	128.7
C_{14}	131.08	131.78	C_{13}	129.90	130.76	130.49	131.27	122.5	127.0
C_9	129.55	130.35	C_7	127.32	128.64	128.43	129.49	121.3	124.9
C_1	128.50	130.09	C_8	126.60	127.91	127.55	129.00	121.3	124.9
C_8	127.20	128.11	C_1	116.18	117.43	121.69	122.77	114.1	115.2
H_6	8.79	9.09	H_{19}	8.79	8.89	8.79	8.99		–
H_{13}	7.76	7.83	H_{10}	8.40	8.53	8.08	8.18	7.76	
H_{15}	7.61	7.73	H_{12}	7.85	7.97	7.73	7.85	7.76	
H_{16}	7.59	7.69	H_4	7.64	7.81	7.61	7.75	7.74	7.70
H_5	7.57	7.64	H_5	7.56	7.64	7.56	7.64	7.72	7.35
H_{11}	7.51	7.62	H_{14}	7.52	7.56	7.51	7.59	7.69	
H_{19}	7.44	7.49	H_{15}	7.51	7.55	7.47	7.52	7.69	
H_4	7.32	7.36	H_{18}	7.29	7.38	7.30	7.37	7.42	

[a,b] These values are the average values of both tautomer for two basis sets.

7. Conclusions

In this work, the 4-phenylimidazole and its tautomer have been characterized by NMR, IR and Raman spectroscopy and NBO analysis. The energies, geometric parameters, vibrational frequencies and $^{13}C/^{1}H$ chemical shift values of the title compounds were calculated using B3LYP with 6-311G(d,p) basis set. For the molecule studied, the tautomer 2 is more stable than tautomer 1 by 5.27 kJ mol^{-1}. Comparison between the calculated geometric and the X-ray structure of the 4-PI molecule show excellent agreement except for some small differences in the C–H bond distances. The experimental infrared and Raman spectra of 4-PI have been assigned and were supported by the calculated (scaled) vibrational spectra. Correlations between the proton and carbon-13 experimental chemical shifts and the GIAO NMR calculations are in good agreement and these values have been used for the definitive signal assignments to the corresponding structural tautomers.

Acknowledgements

This work was supported by the Research Fund of Ahi Evran University Project Number: A10/2009. We would like to thank the central laboratory of METU (ODTÜ) for recording FT-Raman spectra, Gazi University Art and Science Faculty Department of Chemistry for recording FT-IR spectra and Assoc. Prof. Dr Mustafa KURT for Gaussian 03W program package.

Appendix A. Supplementary material

Supplementary data associated with this article can be found, in the online version, at doi:10.1016/j.molstruc.2011.01.001.

References

[1] S.O.P. Kuzmonovic, L.M. Leovac, N.V. Perisicjanjic, J. Rogan, J.J. Balaz, Serb. Chem. Soc. 64 (1999) 381–388.
[2] I.S. Ahuja, I. Prasad, Inorg. Nucl. Chem. Lett. 12 (1976) 777–784.
[3] M.J. Frisch et al., Gaussian 03, Revision C.02, Gaussian, Inc., Wallingford, CT, 2004.
[4] M.H. Jamroz, Vibrational Energy Distribution Analysis VEDA 4, Warsaw, 2004.
[5] A.P. Scott, L. Radom, J. Phys. Chem. 100 (1996) 16502–16513.
[6] E.D, Glendening, A.E. Reed, J.E. Carpenter, F. Weinhold, NBO Version 3.1, TCI, University of Wisconsin, Madison, 1998.
[7] A.E. Reed, L.A.F. Curtiss, Chem. Rev. 88 (1988) 899–926.
[8] R. Ditchfield, J. Chem. Phys. 56 (1972) 5688.
[9] K. Wolinski, J.F. Hinton, P. Pulay, J. Am. Chem. Soc. 112 (23) (1990) 8251–8260.
[10] N. Azizi, A.A. Rostami, A. Godarzian, J. Phys. Soc. Jpn. 74 (2005) 1609–1620.
[11] M. Rohlfing, C. Leland, C. Allen, R. Ditchfield, Chem. Phys. 87 (1984) 9–15.
[12] G. Keresztury, S. Holly, J. Varga, G. Besenyei, A.Y. Wang, J.R. Durig, Spectrochim. Acta 49A (1993) 2007–2017.
[13] G. Keresztury, J.M. Chalmers, P.R. Griffith, Raman spectroscopy: theory, Handbook of Vibrational Spectroscopy, vol. 1, John Wiley & Sons, Ltd., New York, 2002.
[14] R.M. Claramunt, M.D.S. Maria, L. Infantes, F.H. Cano, J. Elguero, J. Chem. Soc., Perkin Trans. 2 (2002) 564–568.
[15] C. Ögretir, S. Yarligan, J. Mol. Struct. (Theochem) 425 (1998) 249–254.
[16] P.V. Maye, C.A. Venanzi, Struct. Chem. 1 (1990) 517–521.
[17] M.R. Hockridge, E.G. Robertson, J.P. Simons, Chem. Phys. Lett. 302 (1999) 538–548.
[18] N. Sundaraganesan, S. Illakiamani, P. Subramani, B.D. Joshua, Spectrochim. Acta 67A (2007) 628–635.
[19] G. Varsanyi, Assignments of Vibrational Spectra of Seven Hundred Benzene Derivatives, vol. 1–2, Adam Hilger, 1974.
[20] G. Socrates, Infrared and Raman Characteristic Group Frequencies: Tables and Charts, third ed., John Wiley & Sons, Ltd., Chichester, 2001.
[21] R.I. Castillo, L.A.R. Montalvo, S.P.H. Rivera, J. Mol. Struct. 877 (2007) 10–19.
[22] N. Sundaraganesan, H. Saleem, S. Mohan, Spectrochim. Acta 59A (2003) 2511–2517.
[23] M.K. Subramanian, P.M. Anbarasan, V. Ilangovan, N. Sundaraganesan, Mol. Simulat. 34 (2008) 277–287.
[24] S. Gunasekaran, S.R. Varadhan, K. Manoharan, Asian J. Phys. 2 (3) (1993) 165–172.
[25] S. Gunasekaran, R. Thilak Kumar, S. Ponnusamy, Spectrochim. Acta 65 (2006) 1041–1052.
[26] N. Sundaraganesan, E. Kavitha, S. Sebastian, J.P. Cornard, M. Martel, Spectrochim. Acta 74A (2009) 788–797.
[27] T. Shimanouchi, Y. Kakiuti, I.J. Gamo, Chem. Phys. 25 (1956) 1245–1251.
[28] R.J. Jakobsen, F.F. Bentely, Appl. Spectrosc. 18 (1964) 88–92.
[29] A.J. Mansingh, Chem. Phys. 52 (1970) 5896–5902.
[30] L. Verdonok, G.P. van Der Kelen, Z. Eeckhant, Spectrochim. Acta 28A (1972) 51–54.
[31] A.P. Datin, J.M. Lebas, Spectrochim. Acta 25A (1969) 168–185.
[32] M. Silverstein, G.C. Basseler, C. Morill, Spectrometric Identification of Organic Compounds, Wiley, New York, 1981.
[33] R. Shanmugam, D. Sathyanarayanan, Spectrochim. Acta 40A (1984) 757–761.
[34] C. James, A.A. Raj, R. Reghunathan, I.H. Joe, V.S. Jayakumar, J. Raman Spectrosc. 37 (2006) 1381–1392.
[35] L. Jun-na, C. Zhi-rang, Y.J. Shen-fang, Zhejiang Univ. Sci. 6B (2005) 584–589.
[36] M. Begtrup, Acta Chem. Scand. 27 (1973) 3101–3110.
[37] K.G.R. Pachler, R. Pachter, P.L. Wessels, Org. Magn. Reson. 17 (1981) 278–284.
[38] A. Koskinen, Heterocycles 19 (1982) 1633–1635.
[39] C. Kashima, Y. Harada, A. Hosomi, Heterocycles 35 (1993) 433–440.
[40] H.O. Kalinowski, S. Berger, S. Braun, C^{-13} NMR Spectroscopy, John Wiley & Sons, Chichester, 1988.
[41] K. Pihlaja, E. Kleinpeter, Carbon^{-13} Chemical Shifts in Structural and Stereo Chemical Analysis, VCH Publishers, Deerfield Beach, FL, 1994.
[42] Y. Erdogdu, M.T. Güllüoğlu, M. Kurt, J. Raman Spectrosc. 40 (2009) 1615–1623.